The ecologist's guide to microclimate modelling and thermal biology in R

Ilya M. D. Maclean[1,*], Lydia G. Soifer[2], David Klinges[3]

[1]Environment and Sustainability Institute, University of Exeter Penryn Campus, Penryn TR10 9FE, United Kingdom. i.m.d.macleam@exeter.ac.uk

[2]School of Natural Resources and Environment, University of Florida, Gainesville, FL, USA

[3]School of the Environment, Yale University, New Haven, Connecticut, USA

*Author for correspondence

Abstract

Many ecological studies relate organismal responses to climate, but available datasets are often poor surrogates for the conditions experienced in nature. Microclimate models address this limitation by translating standard meteorological data into estimates of local temperature, humidity, and radiation at the scales relevant to organisms. Here, we provide a practical guide to mechanistic microclimate modelling and thermal biology in R. We describe how to implement models that estimate microclimatic conditions across habitats, including above, within, and below vegetation canopies and in soils, and how these can be linked to organismal energy balance models to quantify how environmental conditions shape organismal heat exchange and body temperature. The guide is supported by a tutorial, detailed supplementary material, and associated R packages (*microclimlearn* and *micropoint*), providing a practical route for integrating microclimate and thermal biology into ecological analyses and for developing process-based predictions of species' responses to climate.

Key words: *Biophysical ecology, Mechanistic modelling, process-based modelling, Ecophysiology, Ecological forecasting, Tutorial*

Glossary

Albedo. The proportion of incoming solar radiation that a surface reflects back into the atmosphere. Albedo ranges from 0 to 1, where 0 means all radiation is absorbed and 1 means all radiation is reflected. Dark surfaces such as forests usually have low albedo, whereas snow and pale rock have high albedo.

Boundary layer. A thin layer of relatively still air adjacent to a surface or organism through which heat, water vapour, and other gases must diffuse before mixing with the surrounding air. Boundary layer thickness depends mainly on wind speed and surface characteristics, and strongly influences rates of heat and mass exchange.

Diabatic correction coefficients. Adjustment terms used in aerodynamic equations to account for the effects of atmospheric stability on turbulence and heat transfer. They modify wind and temperature profiles under stable or unstable conditions.

Emissivity. A measure of how effectively a surface emits thermal (longwave infrared) radiation relative to an ideal emitter called a black body. Emissivity ranges from 0 to 1. Most natural surfaces, including vegetation and soil, have high emissivity values (typically >0.9).

Energy balance. The balance between rates of energy gain, energy loss, and heat storage within a system. For organisms and surfaces, energy is exchanged through radiation, sensible heat exchange, latent heat exchange, metabolism, and heat storage. Under steady-state conditions the balance sums to zero at the temperature where energy gains equal energy losses.

Forced convection. Heat transfer between a surface and the surrounding fluid driven by externally generated fluid movement, such as wind or flowing water. Stronger airflow generally increases the rate of heat exchange.

Free convection. Heat transfer driven by buoyancy forces that arise because warm fluid is less dense than cold fluid. For example, air warmed by a hot surface rises and is replaced by cooler air.

Heat exchange surface. A hypothetical surface representing the effective level at which a vegetation canopy or other surface exchanges heat, water vapour, and momentum with the atmosphere. It is typically located close to the top of the canopy rather than at the ground surface itself.

Latent heat. Energy absorbed or released during a change in state of water, such as evaporation, condensation, freezing, or melting. In microclimate systems, evaporation removes heat from surfaces and organisms because energy is used to convert liquid water to vapour.

Latent heat of vaporisation. The energy required per unit mass to convert water from liquid to vapour without changing its temperature.

Roughness length for heat. A parameter describing the effective height above a surface at which air temperature is theoretically equal to the surface temperature when extrapolating the vertical temperature profile. It reflects the efficiency of heat transfer between the surface and the atmosphere.

Roughness length for momentum. A parameter describing the effective height above a surface at which wind speed theoretically becomes zero when extrapolating the vertical wind profile. It reflects the aerodynamic roughness of the surface and depends on features such as vegetation height and structure.

Saturation vapour pressure. The maximum water vapour pressure that air can hold at a given temperature. Saturation vapour pressure increases strongly with temperature, which is why warm air can hold more moisture than cold air.

Sensible heat. Heat energy exchanged between a surface and the surrounding air that causes a change in temperature and can be measured directly with a thermometer. Sensible heat transfer occurs mainly through conduction and convection.

Specific heat capacity. The amount of energy required to raise the temperature of a unit mass (typically kg) of a substance by 1 °C (or 1 K). It describes how much energy a material needs to warm up. Materials with high specific heat capacity, such as water, warm and cool more slowly than materials with low specific heat capacity.

Volumetric heat capacity. The amount of energy required to raise the temperature of a unit volume (typically m^3) of a material by 1 °C (or 1 K). Volumetric heat capacity equals specific heat capacity multiplied by density, and therefore describes how much heat can be stored within a given volume of soil, vegetation, water, or air.

Zero-plane displacement height. The height above the ground at which wind flow effectively interacts with a vegetation canopy or rough surface. Within tall vegetation, airflow behaves as though the ground surface were displaced upward to this level.

Introduction

Climatic conditions influence strongly how organisms function. Temperature, humidity and radiation constrain physiological performance and regulate the rates of biological and ecological processes (Angilletta Jr, Steury & Sears 2004). Many ecological studies therefore rely on climate data. However, the climate datasets often used by ecologists, which originate from weather stations, are poor surrogates for the conditions experienced by organisms in nature (Kearney & Porter 2009; Kemppinen *et al.* 2024). Weather stations are designed to measure standardized atmospheric conditions: sensors are shaded from direct sunlight and positioned 1–2 m above the ground in open terrain with free airflow (WMO 2008). These measurements are invaluable for meteorology but can differ substantially from conditions experienced by organisms in natural habitats, which may occur near the ground, within vegetation, or in direct sunlight, often under very different wind conditions from those measured at weather stations (Bramer *et al.* 2018). Weather-station data therefore provide only a crude proxy of the microclimates that shape ecological processes. Estimating microclimatic conditions is increasingly recognised as important for understanding how organisms interact with climate (Briscoe *et al.* 2023; Kemppinen *et al.* 2024).

The physical principles required to estimate microclimate are well established. Many of the equations used today originate from early developments in numerical weather prediction (Richardson 1922) and were later formalised into a general framework describing how temperature, humidity and wind vary near the Earth's surface (Monin & Obukhov 1954). These ideas were widely adopted in agricultural science, where understanding energy and water exchange between land and atmosphere is essential for modelling evapotranspiration (Penman 1948; Monteith 1965). Similar formulations have been extensively developed in meteorology and hydrology and underpin land-surface schemes used in atmospheric models (e.g. Ogée *et al.* 2003; Best *et al.* 2011; Flerchinger *et al.* 2015; Chen *et al.* 2016; Lawrence *et al.* 2019). The same principles also provide a powerful way to understand how organisms interact with their thermal environment. Microclimate estimates provide a basis for predicting body temperature in ectothermic organisms (Gardner *et al.* 2024). This makes it possible to estimate thermal stress, activity windows and performance constraints directly (R. Kearney 2013; Lawrence *et al.* 2019). For endotherms, similar approaches can estimate the energetic costs of thermoregulation (Kearney *et al.* 2021). In both cases, microclimate modelling provides a mechanistic link between environmental conditions and physiological performance that cannot be obtained from ambient climate data alone (Kearney & Porter 2009; Briscoe *et al.* 2023).

Despite the long history of mechanistic microclimate modelling, uptake in ecology has been relatively slow. Ecological studies have often focused on large-scale climate patterns or direct measurement of local conditions and commonly rely on statistical models relating species distributions or demographic rates to macroclimate variables (e.g. Elith & Leathwick 2009; Pigot *et al.* 2023; Sunil *et al.* 2023). Bridging the gap between macroclimate and the microclimates experienced by organisms has only recently gained wider attention (Kemppinen *et al.* 2024). Statistical (Lembrechts *et al.* 2022) or machine learning (Haesen *et al.* 2021) interpolation of observations are often used for estimating microclimate, despite well-known limitations when extrapolating across space or time. A growing range of models and tools now makes it feasible for ecologists to estimate microclimatic conditions and apply biophysical approaches in their own research (e.g. Kearney & Porter 2017; Buckley *et al.* 2023; Maclean 2026). These methods move analysis beyond describing correlations towards identifying the processes that generate ecological responses to climate. While the physical principles underlying such approaches are described in classic texts such as Campbell & Norman (2012) and Gates (2012), much less guidance is available on estimating the microclimatic conditions experienced below or within vegetation canopies, where most terrestrial organisms reside. Additionally, these texts also do not provide code, creating a substantial barrier to uptake and application.

To help address these gaps, we provide a practical guide for ecologists interested in modelling microclimate and organismal energetics in R. The main text introduces the key concepts needed to begin using these approaches, while a more detailed mathematical treatment and extended explanation are provided in the Supporting Information. The Supplementary Information is organised into a series of sections (Notes 1, 2, etc.), each of which is explicitly referenced in the main text to direct readers to

additional detail and equations where required. Where useful, we include a small number of equations in the main text to clarify underlying processes. The main text begins by explaining the principles of microclimate modelling and outlining the overall approach. We then introduce the concept of energy conservation before describing each component in more detail (absorbed and emitted radiation, sensible heat, latent heat, heat storage rate), explaining how these principles can be extended to microenvironments, plants, and animals. Throughout, we provide cross-references to an accompanying tutorial and the associated R package, `microclimlearn`, whose functions are used in the tutorial and referenced in the main text. The tutorial also introduces a range of existing microclimate modelling packages, demonstrating how more comprehensive analyses can be conducted. Together, the main text, supporting material, tutorial, and software provide a practical starting point for ecologists seeking to incorporate microclimate and thermal biology into their research.

General approach

Microclimate modelling is not simply a matter of representing macroclimate at finer spatial resolution (Klinges *et al.* 2024). In contrast to approaches that interpolate or statistically downscale coarse climate data to finer resolution, mechanistic microclimate models resolve the physical processes governing energy balance at or near to surfaces and therefore provide estimates of climatic conditions that potentially differ substantially from standard free-air measurements regardless of spatial scale. Approaches focused on mesoclimate interpolation remain valuable for some applications (see e.g. the mesoclim package; Maclean & Mosedale 2026)), but they are not the focus here.

The general microclimatic modelling process begins by defining what is being modelled. This may be microclimatic conditions above or within the canopy, or below the ground surface, or the thermal environment of an organism itself, such as the body temperature of an ectotherm or heat stress in an endotherm. Each case requires a slightly different treatment.

To model conditions above a vegetation surface, the starting point is usually to estimate the temperature of the canopy ‘heat exchange surface’, a hypothetical surface that enables the ground or vegetated to be treated as a planar surface that exchanges heat with the overlying air (Monteith & Unsworth 2013). Microclimatic conditions at this surface can be modelled from meteorological inputs (typically hourly weather data) together with information on ground surface roughness or vegetation structure, such as canopy height and leaf area. Once the temperature of the heat exchange surface is estimated, vertical profiles in air temperature and humidity above the vegetation can be derived using relatively simple equations.

Within canopies, modelling microclimatic conditions becomes more complicated because the temperature and humidity of air at a given height are influenced by the aggregate exchanges of energy at leaf surfaces throughout the canopy (Raupach 1989a; Raupach 1989b; Monteith & Unsworth 2013; Bonan *et al.* 2021). Modelling therefore requires estimating how these fluxes vary throughout the canopy and in practise is achieved by dividing the canopy into multiple layers and calculating the exchanges of heat or vapour for each layer. At the ground surface, conditions depend on how much sunlight penetrates to the surface and how efficiently heat is transferred to the air, which is largely controlled by wind speed. Below the surface, temperatures follow a predictable phase shift and damping with depth, determined by soil physical properties and water content.

Ground surface and below-ground temperatures are influenced strongly by the storage of heat, which buffers and delays diurnal and annual cycles in energy supply and heat release from the ground. Modelling these conditions therefore requires accounting for the exchange and storage of heat within the soil profile and its coupling to soil moisture dynamics. These processes can be represented using coupled models of soil heat and moisture dynamics based on soil physical properties (e.g. Bittelli, Campbell & Tomei 2015), although simpler approximations are often sufficient in practice (De Vries & Van Wijk 1963; Allen *et al.* 1998; Campbell & Norman 2012).

These microclimatic conditions provide the inputs for modelling the thermal state of organisms (Gardner *et al.* 2024). For ectotherms, this is typically their body temperature, additionally determined by factors such as size, shape, colour and posture. For endotherms, the focus is usually on heat balance

and potential heat stress, which, in addition to these factors, requires representing insulation (fur or feathers) and mechanisms of heat loss such as panting or sweating (Kearney *et al.* 2021).

Because the equations governing microclimate processes are non-linear, mechanistic models are typically run at short time steps (most commonly hourly). If inputs are averaged over longer periods, the resulting estimates are biased because the response to average conditions differs from the average response to varying conditions (Jensen's inequality). Models therefore require meteorological inputs at the same temporal resolution, including air temperature, humidity, wind speed and downward shortwave radiation, and, where available, precipitation, pressure, wind direction, and diffuse and longwave radiation. These are combined with information on terrain (e.g. slope and aspect), soil physical properties, and vegetation characteristics, of which canopy height and leaf area are usually the most important. Where organism temperature or heat balance is modelled, additional trait information is required, depending on whether ectotherms or endotherms are being considered (Kearney & Porter 2020; Kearney *et al.* 2021).

The basics: conservation of energy

The temperatures of organisms and the microenvironments in which they reside are determined by the balance between energy gained and energy lost to their surroundings (Penman 1948; Monteith 1965; Gates 2012). This can be expressed as

$$R_{abs} - R_{em} + M = H + L + G$$

where R_{abs} is absorbed radiation, R_{em} emitted radiation, M the supply of energy to the surface by metabolism (or the absorption of energy during photosynthesis), H is the rate of sensible heat exchange, L is the rate of latent heat exchange and G is the rate of heat storage (or release if negative). In simple terms, the equation states that energy gained from radiation and metabolism must be balanced by energy lost through heat exchange, evaporation, or storage / release.

The individual terms in this equation can be calculated using well-established physical relationships. Absorbed radiation includes shortwave radiation from the sun and longwave (thermal) radiation emitted by the sky and surrounding surfaces, which is why surfaces exposed to direct sunlight, such as rocks or bare ground, become noticeably warmer than those in shade (Bennie *et al.* 2008).

All surfaces also emit thermal radiation as a function of their temperature in accordance with the Stefan–Boltzmann law

$$R_{em} = \varepsilon\sigma\mathbf{T}^4$$

where, ε is the emissivity of the object (0.95-1 for soils, vegetation and most organisms), σ the Stefan-Boltzmann constant ($5.67\text{x}10^{-8}$ $W{\cdot}m^{-2}{\cdot}K^{-4}$) and $\mathbf{T}$ absolute temperature (in Kelvin). This relationship simply states that warmer surfaces emit more thermal radiation than cooler ones and is the mechanism that allows infrared thermal cameras to estimate surface temperatures. It also explains why clear nights are often colder than cloudy nights because clouds emit longwave radiation back towards the surface (Gallo *et al.* 2011).

M represents metabolic heat production, namely energy generated internally by biochemical processes such as metabolism and muscular activity which can be important for endotherms but is usually small for ectotherms. For plants this term represents biochemical energy exchange associated with photosynthesis and respiration, and is typically negligible in the energy balance of individual leaves (Gates 1968).

The net remaining energy is then partitioned into sensible and latent heat or used up (or released) in heat storage. Sensible heat exchange describes the transfer of heat between objects and the surrounding air as a result of a temperature difference. It is derived from Fourier's law of heat transport

$$H = \frac{\hat{\rho} c_p}{r_{HA}} (\mathbf{T}_s - \mathbf{T}_a)$$

where $\hat{\rho}$ and c_p are the density and specific heat of air respectively, r_{HA} is the resistance to heat transfer and $\mathbf{T}_s$ and $\mathbf{T}_a$ the temperature (Kelvin) of the object and the air, respectively. The terms $\hat{\rho} c_p$ together quantify the volumetric heat capacity of air, which largely acts as a unit-conversion factor that relates the difference between surface and air temperature to a heat flux ($W \cdot m^{-2}$) (see functions `rhoair` and `cpair` in the tutorial). The resistance term r_{HA} describes how easily heat is transferred between the surface and the air, which depends mainly on airflow and surface properties (Lhomme 1991). The sensible heat flux therefore increases both when the temperature difference between the surface and the air becomes larger and when wind reduces the resistance to heat transfer – as is intuitively illustrated by the wind chill effect, in which increased wind speed enhances the rate of heat loss.

Conceptually, latent heat can be thought of as energy absorbed or released during phase changes involving water and ice and snow, namely evaporation, condensation, sublimation, or deposition. For example, evaporation cools wet skin because energy is required to convert liquid water to vapour. Latent heat exchange is given by

$$L = \frac{\lambda \hat{\rho}}{r_v p_A} (e_s - e_a)$$

where λ is the latent heat of vaporization, r_v the resistance to vapor exchange, p_A is atmospheric pressure, and e_s and e_a the vapour pressure of the surface and the air, respectively. In simple terms, this equation describes the energy required for a given unit of water to evaporate. Evaporation occurs when the air is drier than the surface, and the rate increases as this difference in vapour pressure between the air and surface becomes larger (Penman 1948). The resistance term r_v reflects how easily water vapour can escape from the surface, which depends on factors such as airflow or stomatal opening in leaves (Farquhar & Sharkey 1982). The remaining terms primarily convert this rate of evaporation into an energy flux.

The G term depends on how the system is being modelled. If heat storage is ignored, $G = 0$, and the energy balance is assumed to be in steady state, such that energy gains and losses are balanced at each time step. This approximation is often appropriate for small organisms and plant leaves, which have little thermal mass and therefore respond rapidly to changing environmental conditions (Porter & Gates 1969). Because components of the energy balance depend on surface temperature, the equilibrium temperature can be found by solving for the temperature at which energy gains and losses are equal (Fig. 1). Larger organisms and environmental surfaces, however, can store substantial amounts of heat, meaning that temperature changes through time must be represented explicitly. In these cases, rather than solving temperature as a fully transient process (in which temperature changes are not assumed to be instantaneous), it is often convenient to define G to represent the imbalance between energy gains and losses as a rate of heat storage or release, allowing temperatures at each time step to be derived using the same equilibrium approach as for steady-state conditions (Campbell & Norman 2012).

This energy balance approach provides a useful starting point for microclimate modelling. With a set of standard weather variables and some basic knowledge of the environment, it can be used to calculate the temperature of a vegetated, animal, or ground surface. To solve the energy balance, one can use a numerical approach, in which a range of candidate temperatures are evaluated. Alternatively, the balance can be solved analytically by linearising the temperature-dependent terms. A widely used formulation is the Penman–Monteith equation (Penman 1948; Monteith 1965), originally developed to estimate evapotranspiration but which also yields surface temperature. This approach is outlined in Note 1. Although analytical solutions introduce small errors, they are computationally far more efficient. In the first section of the tutorial both approaches are illustrated using the `SolveEnergyBalance` function. We use this function to develop a very simple microclimate model, deriving a time-series of canopy surface temperature.

Once the temperature of the surface is known, a simple set of equations are used to derive air temperature or humidity at a given height above canopy (Note 3.2; Fig 2). Similar concepts can be extended to below-canopy (Note 3.3). Together, these provide a first step towards quantifying an organism's microenvironment. By incorporating local modifications to the energy balance (e.g. shading), these conditions can then be used to estimate ectotherm body temperature (Gardner *et al.* 2024) or the metabolic or evaporative costs of thermoregulation in endotherms (Porter & Kearney 2009). Subsequent sections describe how the components of the energy balance can be calculated for organisms and their environments. Table 1 summarises the main controls on each component of the energy balance across microclimates and organisms and acts as a general reference guide

Radiation

Radiation reaching a surface can be divided into two components (Iqbal 2012). The first is shortwave radiation from the sun, which arrives either as direct radiation travelling in a straight line from the sun or as diffuse radiation that has been scattered by particles, clouds, or surrounding objects. The second is thermal (longwave) radiation emitted by the atmosphere and surrounding surfaces, such as vegetation or soil. Any radiation intercepted by an opaque surface is either absorbed or reflected, with the term albedo used to specify the fraction of incoming shortwave (solar) radiation that is reflected by a surface rather than absorbed. Surfaces with a high albedo, such as fresh snow, reflect most of the incoming sunlight, whereas those with a low albedo, such as dark soils, absorb most of it. In a simple microclimate model, the albedo of a vegetated surface is often given a fixed value (e.g. 0.23 for standard well-watered grass surfaces; Allen *et al.* 1998). In reality it is dependent on leaf properties, the angle at which sunlight strikes the surface, the slope and aspect of the underlying ground surface, and how much of the underlying ground is obscured by leaves (Note 2.3). A common solution is to use a two-stream model (Sellers 1985; Yuan *et al.* 2017) to derive albedo as we demonstrate in the tutorial using the aptly named `albedo` function.

The rate of longwave radiation emitted by a surface depends on its temperature and emissivity, which describes how efficiently it emits relative to a perfect emitter (a 'blackbody') at the same temperature. In practice, most natural surfaces such as soil, vegetation and animal tissues have emissivities close to one (Salisbury & D'Aria 1992), meaning they emit thermal radiation almost as efficiently as a blackbody. Conveniently, for opaque surfaces (those that do not transmit radiation), emissivity and longwave reflectivity are related: they sum to one at thermal equilibrium.

Diffuse shortwave and longwave radiation from the sky arrive from many directions and are often treated as approximately isotropic ─ i.e. equal in all directions (Hay & McKAY 1985). The amount absorbed by a surface therefore depends on how much of the sky hemisphere is visible from that surface. For example, a flat, open surface receives radiation from most of the sky, whereas a surface in a steep valley or beside tall terrain receives less radiation from the sky because part of the sky hemisphere is obstructed by surrounding landforms. At the same time, surrounding terrain reflects shortwave radiation and emits thermal radiation toward the surface, so that radiation exchange occurs with both the sky and nearby surfaces. This effect is commonly quantified using the sky view factor, which represents the fraction of the sky hemisphere visible from a given location.

Direct radiation absorbed by a surface depends on the orientation of the surface relative to the position of the sun. Following Bennie *et al* (2008) this can be calculated using a simple extension of Lambert's cosine law in which the fraction of radiation intercepted by a surface is related to the slope and aspect of the surface and solar zenith and azimuth angles (see Note 2.2 and the `sunposition` and `solarindex` functions in the tutorial). In essence, a surface facing the sun intercepts more radiation than one tilted away from it, rather like shining a torch onto a wall: when the beam strikes the surface directly the light is concentrated, but when it hits at a shallow angle the same light is spread over a larger area. In the same way, equatorward-facing slopes intercept more direct radiation than poleward-facing slopes at the same time of day and therefore tend to be warmer. The processes described above are demonstrated in the tutorial in which the `calcRabs` function is used to generate a time-series of radiation absorbed by a canopy for given set of vegetation and weather inputs.

For objects with complex shapes, such as animal bodies, direct radiation must be averaged across the entire surface, which can be cumbersome using Lambert's law directly. This can be simplified by approximating the body as a simple geometric form (e.g. a cylinder or spheroid; Campbell & Norman 2012) and computing its projected area relative to the total surface area, which determines the average flux over the body (Note 2.5). In the tutorial, these calculations are caried out using the '`silhouette`' function. The projected area is equivalent to the shadow the organism would cast if viewed along the direction of the solar beam, and the larger the shadow, the more radiation is intercepted per unit surface area. For example, a person standing upright facing the evening sun intercepts more radiation than if lying down, consistent with intuition from our earlier torch example, and at the same time casts a long shadow.

Below a canopy, it is also necessary to account for the attenuation of radiation as it passes through foliage. This is commonly described using a formulation similar to Beer's law (Note 2.1; Campbell 1986), in which the downward shortwave radiation is attenuated exponentially at a rate determined by an extinction coefficient. In its simplest form, this coefficient is assigned a constant value, commonly either 0.5 or 1. A value of 0.5 is used to approximate a canopy in which leaves are randomly orientated and the sun is always directly overhead, whereas a value near 1 implies stronger attenuation, as expected with more horizontally oriented foliage or more diffuse illumination (Yuan *et al.* 2017). In reality, these assumptions are only approximate. The amount of radiation absorbed depends on leaf orientation relative to incoming sunlight, and leaves reflect and transmit some radiation rather than absorbing it completely, allowing radiation to be scattered within the canopy. More detailed approaches, such as two-stream radiative transfer models, represent these processes more explicitly by separating radiation moving through the canopy into upward and downward diffuse fluxes and allowing radiation to be scattered between leaves (Note 2.3; Fig. 3). Because it is impractical to treat each leaf individually, canopy structure is usually described statistically using a continuous probability density function representing the distribution of leaf angles within the canopy (Campbell 1990). In practice this is most often represented using an ellipsoidal leaf-angle distribution, defined by a single parameter representing the ratio of vertical to horizontal projections of leaf foliage (Campbell 1990). Values of this parameter therefore describe whether foliage is predominantly horizontal or vertical; canopies with more vertically oriented leaves intercept relatively more radiation when the sun is low in the sky, whereas canopies with more horizontal leaves intercept more when the sun is high overhead. This, in turn, allows radiation absorption by a canopy to be estimated without explicitly calculating the orientation and radiation interception of individual leaves (Note 2.5).

Two-stream models, including the version implemented by the tutorial function `twostream`, are widely applied and adequate for many purposes. However, they do not represent the three-dimensional structure of vegetation, nor the spatial distribution of canopy gaps or forest edges. More sophisticated approaches address this by simulating radiation–vegetation interactions using finite-element methods (Gastellu-Etchegorry *et al.* 2015). These models incorporate 3D vegetation structure—often derived from LiDAR or drone data—to numerically simulate interception, scattering, and absorption of radiation across wavelengths. They can represent radiation transfer at fine spatial scales and estimate within-canopy attenuation in structurally complex vegetation (Duffy *et al.* 2021). In practice, however, they are computationally demanding and therefore slow to run.

Longwave radiation within vegetation is dominated by emission rather than scattering because leaves and other canopy elements have very low reflectance (Salisbury & D'Aria 1992). Radiation therefore comes primarily from three sources: the ground (e.g. soil or litter), canopy elements such as leaves and branches, and the sky. Each emits according to its temperature, but their contributions are a little challenging to calculate because temperatures vary vertically within the canopy (Note 2.4), though a method for doing so is provided in the tutorial (see also Fig 3c). A useful simplification is possible if canopy temperatures vary by only a few degrees and remain well above absolute zero. In this case, emission from the ground and vegetation can be approximated using a single mean canopy temperature, and the radiation reaching a given depth in the canopy can be treated as a combination of radiation

transmitted from above and emission from the canopy itself, with the relative contributions determined by canopy density.

Sensible Heat

Sensible heat is the form of heat exchanged between an organism and its environment, or between different elements of the environment (such as between the canopy surface and the air above it). The temperature of an insect or leaf, for example, is influenced by the temperature of the air surrounding it. The rate at which sensible heat is gained from or lost to the surroundings as a function of the temperature differential is governed by a 'resistance to heat loss'—a term that is inversely related to the conductance for heat transfer (Note 3.1). When heat is transferred through a fluid such as air the process is referred to as convection, but the same relationship applies: resistance is simply the inverse of the conductance governing this exchange. The magnitude of this resistance depends on factors such as wind speed and surface properties.

To understand these processes better it is useful to consider the pathway by which heat reaches the surface of an object and the way in which airflow removes heat from that surface. In endotherms, which metabolically generate heat, internal heat transfer is important as the generated heat must pass from the body core to the surface and it is convenient to treat the pathway of heat loss as a series of resistances, analogous to electrical resistances in a circuit (Porter & Gates 1969). Heat must pass from the vascularised tissue beneath the skin, across the skin surface and any insulating layers such as fur or feathers, and finally through the boundary air layer to the surrounding environment, with the resistance of coats or feathers being much greater than that of the underlying tissues. Simple empirical relationships have been derived relating coat or feather resistance to the thickness of the insulating layer and wind speed (e.g. Calder 1974; Campbell, McArthur & Monteith 1980; Monteith & Unsworth 2013). By contrast, for small ectotherms temperature is often nearly uniform, so it is unnecessary to consider internal heat transfer (Porter & Gates 1969).

At the surface of an organism, at the so-called boundary layer, surface drag results in slow and smooth layered movement of fluid particles in which layers slide past one another rather like playing cards. In this so-called laminar flow, conduction between the surface and the air is simultaneously accompanied by heat transfer across streamlines in the air by molecular diffusion (Bird, Stewart & Lightfoot 2007). These laminar flows can be classed as either forced or free depending on how the air motion is initiated. In free convection, motion is caused by buoyancy—the rise of warmer air and fall of cooler air—generating circular movement rather like heated water in a saucepan. In forced convection, such as occurs in the natural environment due to wind, the transport of heat is also influenced by the velocity of the air. However, as one moves further away from the object, the orderly layered movement breaks down, and flow regimes are characterised by turbulent movements and rapidly fluctuating eddies (Incropera *et al.* 2007). These small whirlpools or vortices transport heat efficiently across the fluid in proportion to the size of the eddies. An entirely first-principles analysis of boundary-layer conductance is extremely challenging and is generally approached by defining dimensionless variables that have been found empirically to correlate with heat transfer. These relationships can then be used to estimate conductance for simple geometric shapes as detailed in Note 3.4.

Convective heat transfer also influences air temperature above soil or above the canopy 'heat exchange surface', the level within the canopy at which it exchanges heat with the atmosphere as a planar surface. At this scale, heat exchange is dominated by turbulent mixing. Because drag slows wind near the surface, wind speed increases approximately logarithmically with height, and the resistance to heat transfer between the canopy and the overlying air depends on wind speed and canopy structure (Garratt & Hicks 1973; Harman & Finnigan 2007). In simple terms, the canopy affects airflow by shifting the effective origin of the wind profile upward (the zero-plane displacement height) and by controlling how rapidly wind speed and turbulent exchange increase with height (through roughness lengths for heat and momentum). These properties can be approximated from canopy height, and more accurately with additional information on vegetation structure (Raupach 1994; see tutorial functions `zeroplanedis`

and `roughlength`). Atmospheric stability further modifies turbulent mixing, and is commonly represented through stability correction functions (Businger *et al.* 1971; Note 2.2; tutorial functions `dpsim`, `dpsih`).

Above the canopy, turbulent mixing produces smooth vertical temperature gradients. Inside the canopy, however, heat transfer cannot be treated as a simple, well-mixed system. Leaves act as distributed sources and sinks of heat, and airflow is uneven, so conditions at any point reflect both local exchanges and the cumulative effects of interactions elsewhere in the canopy. A series of seminal papers (Raupach 1989a; Raupach 1989b) developed a coherent 'localized near-field theory' and practical model for representing these processes. It is assumed that a leaf affects the air immediately around it by heating or cooling it, but this effect weakens rapidly with distance. At the same time, the air at any point also contains the accumulated influence of interactions with many other leaves encountered as it has moved through the canopy. The approach therefore separates these influences into two parts: a local 'near-field' contribution from nearby leaves, and a more distributed 'far-field' contribution representing the combined effect of the rest of the canopy. Conditions at a given height are then described as the combination of these local and non-local influences, rather than as the result of a single, uniform canopy environment. The mathematics behind this theory is quite involved, but its practical implementation is more straightforward and is described fully in Note 3.3. The canopy is sub-divided into a series of vertical layers, and the energy balance of each layer is calculated individually. The near-field contribution is determined from the local energy balance of each layer, whereas the far-field represents the combined influence of all other layers, with their contributions weighted according to how effectively heat is transported between layers. The tutorial function `temp_below` applies this theory and Fig. 4 shows an example of the resulting temperature profile.

Latent Heat

Latent heat is the heat exchanged when water changes phase, most commonly during evaporation or condensation. In ecological systems this typically occurs through processes such as evaporation from soil and wet surfaces, and transpiration from plant leaves. The ways in which it is quantified are remarkably similar to sensible heat, except that instead of a temperature differential it is a vapour pressure differential that drives the rate of vapour exchange (Monteith 1965; Monteith & Unsworth 2013). The vapour pressure at an evaporating surface is typically close to the saturation vapour pressure at the surface temperature, whereas the air contains some lower amount of water vapour. Because saturation vapour pressure increases strongly with temperature, warmer surfaces tend to create larger vapour pressure differences and therefore greater potential for evaporation. The surface in ecological systems is typically the ground surface, the surface of an organism, or the surface of a leaf. For organisms the rate of evaporation can often be approximated by including a simple term describing the fraction of the surface that behaves as a freely evaporating surface (Note 4.5). For soils evaporation is strongly constrained by soil water content, which determines how readily water can be supplied to the surface (Bittelli, Campbell & Tomei 2015). In plants water vapour exchange occurs primarily through stomata—small pores in the leaf surface that regulate the loss of water vapour from the leaf interior to the surrounding air. This regulation is commonly represented as a stomatal resistance, which acts in addition to the boundary-layer resistance described earlier for sensible heat (Note 4.2).

Leaves regulate water loss by adjusting the opening of stomata in response to environmental conditions. As a result, the resistance to vapour loss from a leaf varies with factors such as photosynthetically active radiation (PAR), leaf water status, atmospheric dryness and temperature. The physiological mechanisms underlying these responses involve complex chemical signalling and hydrodynamic processes within leaf cells, some of which remain incompletely understood (Buckley 2017; Eller *et al.* 2020). Rather than attempting to represent these processes explicitly, models usually estimate stomatal resistance directly from environmental conditions using simplified formulations. One important class of such formulations is based on the Cowan–Farquhar framework, in which stomatal behaviour reflects a balance between carbon gain through photosynthesis and water loss through transpiration (Cowan & GD 1977; Buckley 2017; Dewar *et al.* 2018). The stomatal formulation used in the tutorial examples follows this general approach, using the extension developed by Eller et al. (2020) (see also Note 4.3).

Heat storage and transient temperature dynamics

So far, we have treated energy exchange as if temperature adjusts instantaneously to changes in radiation, convection, and evaporation. As an alternative to defining a rate of heat storage, one can also model transient changes in temperature explicitly (Seebacher, Elsey & Trosclair III 2003). If internal temperature gradients are not important, temperature change over a time step can be estimated directly from the net energy balance, scaled by the amount of material that must be heated (i.e. the ratio of surface area to volume and the heat capacity of the organism). This means that larger organisms, or those with higher heat capacity, change temperature more slowly than smaller ones under the same conditions, which can buffer short-term environmental variation (Pincebourde, Dillon & Woods 2021).

In soils, temperature gradients are almost always important, and heat storage cannot be treated as spatially uniform. Instead, temperature varies with both depth and time as heat is conducted through the soil profile (Bittelli, Campbell & Tomei 2015). Changes at a given depth reflect imbalances in heat flow, and the rate of change depends on both temperature gradients and the soil's volumetric heat capacity (Campbell & Norman 2012). Closed-form solutions exist only for simplified conditions and are rarely applicable in the field, although they provide useful intuition. In practice, soil heat storage is sometimes approximated as a fixed fraction of net radiation (Allen *et al.* 1998), but this ignores temporal dynamics, particularly the lag and damping of temperature with depth (Fig. 5). In reality, with increasing depth belowground, temperature peaks later and with reduced amplitude as heat propagates downward from the surface (Horton & Wierenga 1983; Bittelli, Campbell & Tomei 2015). A more physically grounded closed-form solution is provided by de Vries (1963), who represented surface temperature forcing as sinusoidal and derived expressions for temperature variation with depth and time. This approach assumes a homogeneous, infinitely deep soil, allowing temperature waves to propagate downward with predictable attenuation and phase lag. Although rarely met in practice, it provides useful insight into the damping and delay of temperature signals in soils.

A more general approach is to represent the soil as a series of layers and solve for heat transfer numerically (Bittelli, Campbell & Tomei 2015). This approach allows temperature to vary realistically with depth and time and can accommodate changes in soil properties with depth. In practice, soil thermal properties are strongly influenced by water content, which affects both heat capacity and thermal conductivity. As a result, realistic simulation of soil temperature dynamics typically requires a coupled representation of soil moisture, in which water movement and heat transfer are solved together so that changes in moisture content, and therefore thermal behaviour, are captured through time. Such coupled approaches form the basis of more advanced microclimate models, including implementations described by Bittelli et al (2015) and used in modelling packages such as NicheMapR (Kearney & Porter 2017) (Kearney & Porter, 2017) and presented in the tutorial. However, fully resolving hydrological processes such as lateral water movement, runoff, and groundwater interactions is beyond the scope of this guide. Readers requiring more detailed hydrological treatment are referred to established frameworks such as SWAT (Douglas-Mankin, Srinivasan & Arnold 2010) or standard hydrology texts (e.g. Dingman 2015).

The same principles described for soil apply to any system where internal temperature gradients are important. Large organisms, tree stems, or rocks, for example, can exhibit temperature variation within their structure when heat storage is significant. Unlike the treatments above, which assume spatially uniform temperature, these systems require temperature to be resolved through the material and therefore must be solved numerically by discretising into layers (Kreith, Manglik & Bohn 2012). This introduces a key practical challenge: because heat fluxes depend on temperature gradients, which themselves depend on the evolving temperature profile, the order of calculations within each time step influences the solution. Numerical implementations can therefore be sensitive to time step length and are most robust when run at short time steps.

Snow

In cold environments, snow can strongly modify microclimate by insulating the ground, altering surface energy balance, and decoupling near-surface air and soil temperatures. Representing these effects

requires accounting for snow accumulation, compaction, and melt, as well as the strong dependence of thermal conductivity and albedo on snow properties. As with soil water, these processes are most often handled using layered numerical models. Notes 7.1–7.2 outline the key processes, and the tutorial includes a simple one-dimensional multi-layer snow model. However, detailed treatment of snow physics is beyond the scope of this guide. Readers interested in more comprehensive approaches are referred to established models such as CROCUS (Brun *et al.* 1989) or more detailed treatments of snow physics and surface energy balance in standard texts (Armstrong & Brun 2008).

Concluding remarks

The accompanying tutorial provides a structured walkthrough of the approaches described here, beginning with simple energy balance calculations and progressively building to more complete representations of microclimate above and within canopies, in soils, and under snow. The final section introduces a range of existing software packages, illustrating how these methods are implemented in practice and how more comprehensive analyses can be conducted. Our aim in this paper is not to reproduce the extensive documentation already available for these tools, but to clarify the underlying principles that they share and that are often less explicitly described. The tutorial therefore serves as a practical bridge between these principles and their implementation.

Together, these approaches provide a flexible framework for linking microclimatic conditions to organismal processes across a wide range of environments. While additional complexity can be introduced where required—such as resolving internal temperature gradients or incorporating snow and hydrological dynamics—many ecological questions can be addressed using relatively simple formulations of the energy balance. The key challenge is therefore not the availability of models, but their appropriate application. By focusing on the underlying physical principles and providing a practical route to implementation, we aim to support more widespread and consistent use of microclimate and thermal biology in ecological research.

Acknowledgements

This work was supported by the UK Natural Environment Research Council (NERC) under grant number NE/X015262/1.

Data availability

The code, tutorial materials, and example workflows associated with this manuscript are publicly available through the https://github.com/ilyamaclean/microclimlearn GitHub repository and the accompanying tutorial hosted on https://rpubs.com/ilyamaclean/microclimlearn.

References

Allen, R.G., Pereira, L.S., Raes, D. & Smith, M. (1998) *Crop evapotranspiration-Guidelines for computing crop water requirements*. FAO Irrigation and drainage paper 56. FAO, Rome, 300, D05109.

Angilletta Jr, M.J., Steury, T.D. & Sears, M.W. (2004) Temperature, growth rate, and body size in ectotherms: fitting pieces of a life-history puzzle. Integrative and comparative biology, 44, 498-509.

Armstrong, R.L. & Brun, E. (2008) *Snow and Climate: Physical Processes, Surface Energy Exchange and Modeling*. Cambride University Press.

Bennie, J., Huntley, B., Wiltshire, A., Hill, M.O. & Baxter, R. (2008) Slope, aspect and climate: spatially explicit and implicit models of topographic microclimate in chalk grassland. *Ecological Modelling*, 216, 47-59.

Best, M.J., Pryor, M., Clark, D., Rooney, G.G., Essery, R., Ménard, C., Edwards, J., Hendry, M., Porson, A. & Gedney, N. (2011) The Joint UK Land Environment Simulator (JULES), model description–Part 1: energy and water fluxes. *Geoscientific Model Development*, 4, 677-699.

Bird, R.B., Stewart, W.E. & Lightfoot, E.N. (2007) *Transport Phenomena* (2nd ed.). John Wiley & Sons, New York.

Bittelli, M., Campbell, G.S. & Tomei, F. (2015) *Soil physics with Python: transport in the soil-plant-atmosphere system*. Open University Press, Oxford.

Bonan, G.B., Patton, E.G., Finnigan, J.J., Baldocchi, D.D. & Harman, I.N. (2021) Moving beyond the incorrect but useful paradigm: reevaluating big-leaf and multilayer plant canopies to model biosphere-atmosphere fluxes–a review. *Agricultural and Forest Meteorology*, 306, 108435.

Bramer, I., Anderson, B.J., Bennie, J., Bladon, A.J., De Frenne, P., Hemming, D., Hill, R.A., Kearney, M.R., Körner, C., Korstjens, A.H., Lenoir, J., Maclean, I.M.D., Marsh, C.D., Morecroft, M.D., Ohlemüller, R., Slater, H.D., Suggitt, A.J., Zellweger, F. & Gillingham, P.K. (2018) Advances in monitoring and modelling climate at ecologically relevant scales. *Advances in Ecological Research*, 58, 101–161.

Briscoe, N.J., Morris, S.D., Mathewson, P.D., Buckley, L.B., Jusup, M., Levy, O., Maclean, I.M., Pincebourde, S., Riddell, E.A. & Roberts, J.A. (2023) Mechanistic forecasts of species responses to climate change: the promise of biophysical ecology. *Global Change Biology*, 29, 1451-1470.

Brun, E., Martin, E., Simon, V., Gendre, C. & Coleou, C. (1989) An energy and mass model of snow cover suitable for operational avalanche forecasting. *Journal of Glaciology*, 35, 333-342.

Buckley, L.B., Briones Ortiz, B.A., Caruso, I., John, A., Levy, O., Meyer, A.V., Riddell, E.A., Sakairi, Y. & Simonis, J.L. (2023) TrenchR: An R package for modular and accessible microclimate and biophysical ecology. *PLoS Climate*, 2, e0000139.

Buckley, T.N. (2017) Modeling stomatal conductance. *Plant Physiology*, 174, 572-582.

Businger, J.A., Wyngaard, J.C., Izumi, Y. & Bradley, E.F. (1971) Flux-profile relationships in the atmospheric surface layer. *Journal of the Atmospheric Sciences*, 28, 181-189.

Calder, W. (1974) Thermal and caloric relations of birds. *Avian Biology*, 4, 259-413.

Campbell, G. (1990) Derivation of an angle density function for canopies with ellipsoidal leaf angle distributions. *Agricultural and Forest Meteorology*, 49, 173-176.

Campbell, G., McArthur, A. & Monteith, J. (1980) Windspeed dependence of heat and mass transfer through coats and clothing. *Boundary-Layer Meteorology*, 18, 485-493.

Campbell, G.S. (1986) Extinction coefficients for radiation in plant canopies calculated using an ellipsoidal inclination angle distribution. *Agricultural and Forest Meteorology*, 36, 317-321.

Campbell, G.S. & Norman, J.M. (2012) *An introduction to environmental biophysics*. Springer Science & Business Media.

Chen, Y., Ryder, J., Bastrikov, V., McGrath, M.J., Naudts, K., Otto, J., Ottlé, C., Peylin, P., Polcher, J. & Valade, A. (2016) Evaluating the performance of land surface model ORCHIDEE-CAN v1. 0 on water and energy flux estimation with a single-and multi-layer energy budget scheme. *Geoscientific Model Development*, 9, 2951-2972.

Cowan, I.R. & Farquhar, G.D. (1977) Stomatal function in relation to leaf metabolism and environment. In: *Integration of Activity in the Higher Plant* (ed. D.H. Jennings), pp. 471–505. Cambridge University Press, Cambridge.

Dewar, R., Mauranen, A., Mäkelä, A., Hölttä, T., Medlyn, B. & Vesala, T. (2018) New insights into the covariation of stomatal, mesophyll and hydraulic conductances from optimization models incorporating nonstomatal limitations to photosynthesis. *New Phytologist*, 217, 571-585.

Dingman, S.L. (2015) *Physical hydrology*. Waveland press.

Douglas-Mankin, K., Srinivasan, R. & Arnold, J. (2010) Soil and Water Assessment Tool (SWAT) model: Current developments and applications. *Transactions of the ASABE*, 53, 1423-1431.

Duffy, J.P., Anderson, K., Fawcett, D., Curtis, R.J. & Maclean, I.M.D. (2021) Drones provide spatial and volumetric data to deliver new insights into microclimate modelling. *Landscape Ecology*, 36, 1309–1324.

Elith, J. & Leathwick, J.R. (2009) Species distribution models: ecological explanation and prediction across space and time. Annual Review of Ecology, Evolution, and Systematics, 40, 677-697.

Eller, C.B., Rowland, L., Mencuccini, M., Rosas, T., Williams, K., Harper, A., Medlyn, B.E., Wagner, Y., Klein, T. & Teodoro, G.S. (2020) Stomatal optimization based on xylem hydraulics (SOX) improves land surface model simulation of vegetation responses to climate. *New Phytologist*, 226, 1622-1637.

Farquhar, G.D. & Sharkey, T.D. (1982) Stomatal conductance and photosynthesis. *Annual Review of Plant Physiology*, 33, 317-345.

Flerchinger, G.N., Reba, M.L., Link, T.E. & Marks, D. (2015) Modeling temperature and humidity profiles within forest canopies. *Agricultural and Forest Meteorology*, 213, 251-262.

Gallo, K., Hale, R., Tarpley, D. & Yu, Y. (2011) Evaluation of the relationship between air and land surface temperature under clear-and cloudy-sky conditions. *Journal of Applied Meteorology and Climatology*, 50, 767-775.

Gardner, A.S., Maclean, I.M., Rodríguez-Muñoz, R., Hopwood, P.E., Mills, K., Wotherspoon, R. & Tregenza, T. (2024) The relationship between the body and air temperature in a terrestrial ectotherm. *Ecology and Evolution*, 14, e11019.

Garratt, J. & Hicks, B. (1973) Momentum, heat and water vapour transfer to and from natural and artificial surfaces. *Quarterly Journal of the Royal Meteorological Society*, 99, 680-687.

Gastellu-Etchegorry, J.-P., Yin, T., Lauret, N., Cajgfinger, T., Gregoire, T., Grau, E., Feret, J.-B., Lopes, M., Guilleux, J. & Dedieu, G. (2015) Discrete anisotropic radiative transfer

(DART 5) for modeling airborne and satellite spectroradiometer and LIDAR acquisitions of natural and urban landscapes. *Remote Sensing*, 7, 1667-1701.

Gates, D.M. (1968) Transpiration and leaf temperature. *Annual Review of Plant Physiology*, 19, 211-238.

Gates, D.M. (2012) *Biophysical Ecology*. Dover Publications, Mineola, NY.

Haesen, S., Lembrechts, J.J., De Frenne, P., Lenoir, J., Aalto, J., Ashcroft, M.B., Kopecký, M., Luoto, M., Maclean, I. & Nijs, I. (2021) ForestTemp–Sub-canopy microclimate temperatures of European forests. *Global Change Biology*, 27, 6307-6319.

Harman, I.N. & Finnigan, J.J. (2007) A simple unified theory for flow in the canopy and roughness sublayer. *Boundary-layer Meteorology*, 123, 339-363.

Hay, J.E. & McKay, D.C. (1985) Estimating solar irradiance on inclined surfaces: a review and assessment of methodologies. *International Journal of Solar Energy*, 3, 203-240.

Horton, R. & Wierenga, P. (1983) Estimating the soil heat flux from observations of soil temperature near the surface. *Soil Science Society of America Journal*, 47, 14-20.

Incropera, F.P., DeWitt, D.P., Bergman, T.L. & Lavine, A.S. (2007) Fundamentals of Heat and Mass Transfer (6th ed.). John Wiley & Sons, New York.

Iqbal, M. (2012) *An introduction to solar radiation*. Elsevier.

Kearney, M.R. (2013) Activity restriction and the mechanistic basis for extinctions under climate warming. Ecology Letters, 16, 1470-1479.

Kearney, M. & Porter, W. (2009) Mechanistic niche modelling: combining physiological and spatial data to predict species' ranges. *Ecology Letters*, 12, 334-350.

Kearney, M.R., Briscoe, N.J., Mathewson, P.D. & Porter, W.P. (2021) NicheMapR–an R package for biophysical modelling: the endotherm model. Ecography, 44, 1595-1605.

Kearney, M.R. & Porter, W.P. (2017) NicheMapR–an R package for biophysical modelling: the microclimate model. *Ecography*, 40, 664-674.

Kearney, M.R. & Porter, W.P. (2020) NicheMapR–an R package for biophysical modelling: the ectotherm and dynamic energy budget models. *Ecograph*y, 43, 85-96.

Kemppinen, J., Lembrechts, J.J., Van Meerbeek, K., Carnicer, J., Chardon, N.I., Kardol, P., Lenoir, J., Liu, D., Maclean, I. & Pergl, J. (2024) Microclimate, an important part of ecology and biogeography. *Global Ecology and Biogeography*, 33, e13834.

Klinges, D.H., Baecher, J.A., Lembrechts, J.J., Maclean, I.M., Lenoir, J., Greiser, C., Ashcroft, M., Evans, L.J., Kearney, M.R. & Aalto, J. (2024) Proximal microclimate: Moving beyond spatiotemporal resolution improves ecological predictions. *Global Ecology and Biogeography*, 33, e13884.

Kreith, F., Manglik, R.M. & Bohn, M.S. (2012) Principles of heat transfer. Cengage learning.

Lawrence, D.M., Fisher, R.A., Koven, C.D., Oleson, K.W., Swenson, S.C., Bonan, G., Collier, N., Ghimire, B., van Kampenhout, L. & Kennedy, D. (2019) The Community Land Model

version 5: Description of new features, benchmarking, and impact of forcing uncertainty. *Journal of Advances in Modeling Earth Systems*, 11, 4245-4287.

Lembrechts, J.J., Van Den Hoogen, J., Aalto, J., Ashcroft, M.B., De Frenne, P., Kemppinen, J., Kopecký, M., Luoto, M., Maclean, I.M. & Crowther, T.W. (2022) Global maps of soil temperature. *Global Change Biology*, 28, 3110-3144.

Lhomme, J.-P. (1991) The concept of canopy resistance: historical survey and comparison of different approaches. *Agricultural and Forest Meteorology*, 54, 227-240.

Maclean, I.M. (2026) Microclimf: Fast modelling of microclimate across real landscapes in R. *Methods in Ecology and Evolution*, 17, 1112-1123.

Maclean, I.M.D. & Mosedale, J.R. (2026) Climate downscaling and bias correction with R. Available: https://github.com/ilyamaclean/mesoclim/.

Monin, A. & Obukhov, A. (1954) Osnovnye zakonomernosti turbulentnogo peremeshivanija v prizemnom sloe atmosfery (Basic laws of turbulent mixing in the atmosphere near the ground). *Trudy Geofizicheskogo Instituta AN SSSR*, 24, 163–187.

Monteith, J. & Unsworth, M. (2013) *Principles of environmental physics: plants, animals, and the atmosphere*. Academic press.

Monteith, J.L. (1965) Evaporation and environment. Symposia of the society for experimental biology, pp. 205-234. Cambridge University Press (CUP) Cambridge.

Ogée, J., Brunet, Y., Loustau, D., Berbigier, P. & Delzon, S. (2003) MuSICA, a CO2, water and energy multilayer, multileaf pine forest model: evaluation from hourly to yearly time scales and sensitivity analysis. *Global Change Biology*, 9, 697-717.

Penman, H.L. (1948) Natural evaporation from open water, bare soil and grass. *Proceedings of the Royal Society of London. Series A. Mathematical and Physical Sciences*, 193, 120-145.

Pigot, A.L., Merow, C., Wilson, A. & Trisos, C.H. (2023) Abrupt expansion of climate change risks for species globally. *Nature Ecology & Evolution*, 7, 1060-1071.

Pincebourde, S., Dillon, M.E. & Woods, H.A. (2021) Body size determines the thermal coupling between insects and plant surfaces. *Functional Ecology*, 35, 1424-1436.

Porter, W.P. & Gates, D.M. (1969) Thermodynamic equilibria of animals with environment. *Ecological Monographs*, 39, 227-244.

Porter, W.P. & Kearney, M. (2009) Size, shape, and the thermal niche of endotherms. *Proceedings of the National Academy of Sciences*, 106, 19666-19672.

Raupach, M. (1989a) Applying Lagrangian fluid mechanics to infer scalar source distributions from concentration profiles in plant canopies. *Agricultural and Forest Meteorology*, 47, 85-108.

Raupach, M. (1989b) A practical Lagrangian method for relating scalar concentrations to source distributions in vegetation canopies. *Quarterly Journal of the Royal Meteorological Society*, 115, 609-632.

Raupach, M. (1994) Simplified expressions for vegetation roughness length and zero-plane displacement as functions of canopy height and area index. *Boundary-Layer Meteorology*, 71, 211-216.

Richardson, L.F. (1922) *Weather prediction by numerical process*. University Press.

Salisbury, J.W. & D'Aria, D.M. (1992) Emissivity of terrestrial materials in the 8–14 μm atmospheric window. *Remote Densing of Environment*, 42, 83-106.

Seebacher, F., Elsey, R.M. & Trosclair III, P.L. (2003) Body temperature null distributions in reptiles with nonzero heat capacity: seasonal thermoregulation in the American alligator (Alligator mississippiensis). *Physiological and Biochemical Zoology*, 76, 348-359.

Sellers, P.J. (1985) Canopy reflectance, photosynthesis and transpiration. *International Journal of Remote Sensing*, 6, 1335-1372.

Sunil, V., Majeed, W., Chowdhury, S., Riaz, A., Shakoori, F.R., Tahir, M. & Dubey, V.K. (2023) Insect population dynamics and climate change. *Climate change and insect biodiversity*, pp. 121-146. CRC Press.

de Vries, D.A. & van Wijk, W.R. (1963) Physics of plant environment. In: *Environmental Control of Plant Growth* (ed. W.R. van Wijk), pp. 59–109. North-Holland Publishing Company, Amsterdam.Cowan, I.R. & GD, F. (1977) Stomatal function in relation to leaf metabolism and environment.

WMO (2008) *Guide to meteorological instruments and methods of observation* (WMO-No. 8). World Meteorological Organisation: Geneva, Switzerland, 29.

Yuan, H., Dai, Y., Dickinson, R.E., Pinty, B., Shangguan, W., Zhang, S., Wang, L. & Zhu, S. (2017) Reexamination and further development of two-stream canopy radiative transfer models for global land modeling. *Journal of Advances in Modeling Earth Systems*, 9, 113-129.

Table 1. Key determinants of the major energy balance components governing microclimate and organism temperature. For microclimates, macroclimatic forcing interacts with local environmental properties and environmental modification processes to determine near-surface conditions. These resulting microclimatic conditions then form the inputs governing organism energy exchange, with organism traits determining how radiation, heat, and water are exchanged with the surrounding environment.

	Microclimate		**Organism**	
Energy balance component	**Climate determinants**	**Other determinants**	**Environmental modification**	**Organism trait determinants**
Absorbed radiation	Downard longwave and shortwave radiation fluxes, normally provided as inputs to a microclimate model, but dependent on cloud cover. Shortwave radiation is partitioned into its direct and diffuse components.	Vegetation emissivity, which determines longwave radiation absorption, and surface albedo, governed by leaf and ground reflectance, foliage density, terrain slope and aspect, and leaf inclination relative to the sun, which together influence radiation interception.	Vegetative shading. In steep valleys, the sun may fall below the horizon, obscuring direct shortwave radiation and reducing sky view, thereby lowering diffuse and incoming longwave radiation while increasing upward reflected radiation. Leaf and ground reflectance further modify these fluxes.	Surface reflectance (i.e. the colour of the organism). Its emissivity, and its shape and orientation relative to the position of the sun.
Emitted radiation	None.	The emissivity of the surface, which determines how emitted radiation scales with absolute temperature.	A fraction of emitted radiation is absorbed and re-emitted by vegetation of the ground surface.	Organism emissivity.
Sensible heat	Wind speed and the temperature of the air at reference height relative to the surface. Direction important for terrain sheltering.	Vegetation height and foliage density, which influence surface drag and the shape of the wind profile.	Terrain sheltering and reduced wind speeds below or near a vegetated surface reduce resistance to sensible heat loss. Surfaces act as heat sources or sinks influencing microclimate air temperature	Body size and shape. Orientation relative to the direction of wind flow. Surface texture. Behavioural thermoregulation.
Latent heat	Same as sensible heat but with additional dependency on air humidity and pressure.	Same as sensible heat, but additionally influenced by stomatal opening and closure, which regulate transpiration in response to light, humidity, temperature, soil moisture, and atmospheric CO_2 concentration.	Same as for sensible heat, but surfaces act as sources or sinks for vapour fluxes	Skin permeability, sweating or panting capacity, respiratory structure, body size, insulation, and behavioural regulation of water balance.
Rate of heat storage	Downward longwave and shortwave radiation reaching soil surface. Wind speed and air temperature	Soil bulk density and water content. Clay, mineral, quartz and organic content.	N/A	Volume and specific heat capacity, contingent on body composition and water content.

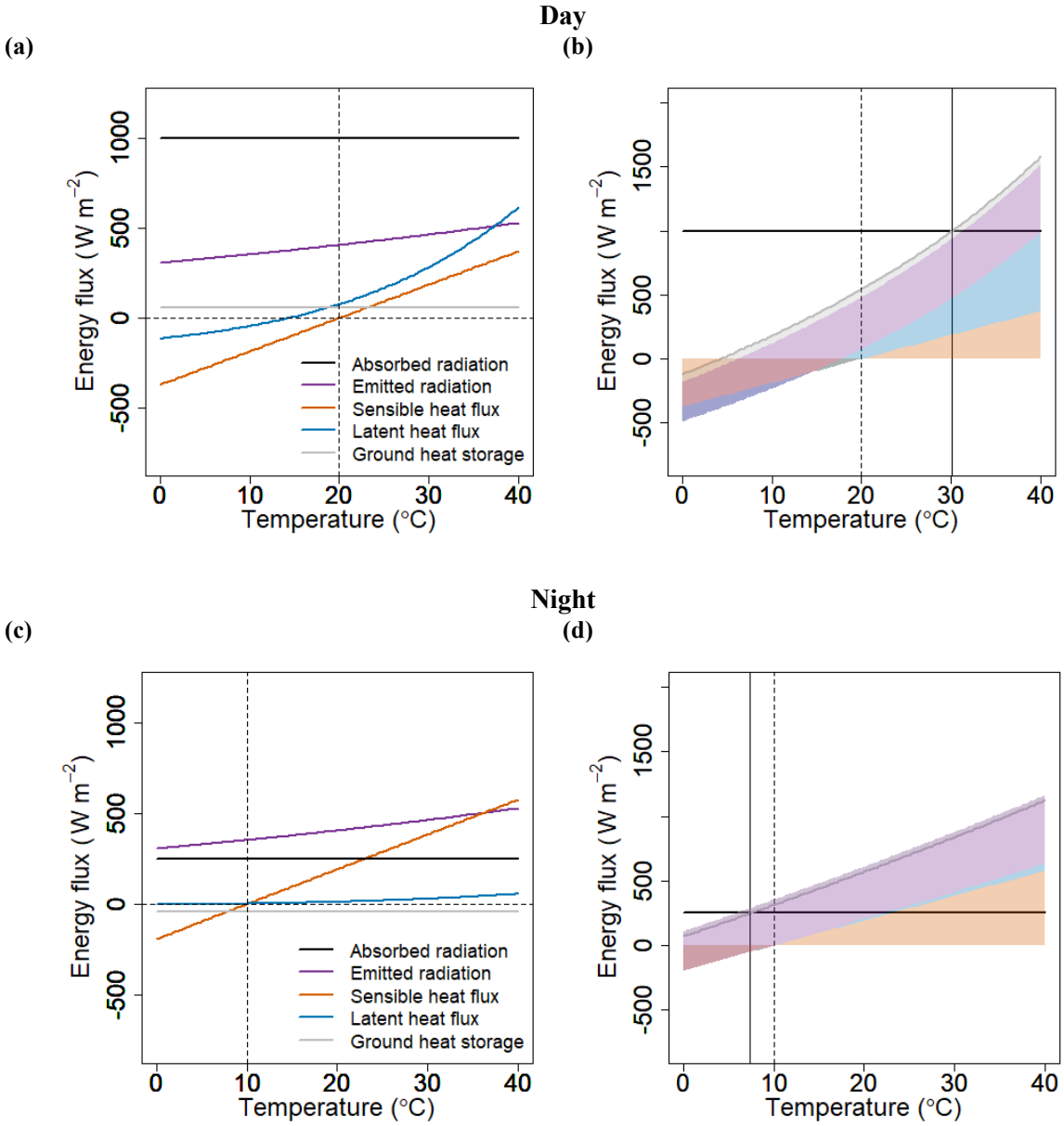

Fig. 1. Energy balance framework used to derive the temperature of a vegetated surface. In (a), the temperature dependence of each energy balance component is shown for typical daytime conditions. Absorbed radiation (black) and the rate of ground heat storage (grey) are treated as fixed inputs; absorbed radiation is typically high under sunshine, while ground heat storage is generally positive during the day. Emitted radiation (purple) increases with temperature. Sensible heat loss (orange) increases linearly with the temperature of the surfaces and is negative (heat gain) when the surface is cooler than the air. Latent heat loss (blue) is negative when the surface is cooler than the air owing to condensation but is generally positive when the surface us warmer than the air (loss of heat by evapotranspiration). However, some evapotranspiration can occur when the surface is slightly below air temperature because of atmospheric vapour pressure deficit. In (b), total incoming (black) and outgoing (grey) energy fluxes are shown as functions of surface temperature. The equilibrium surface temperature (solid vertical line) occurs where the curves intersect. Shading indicates the contribution of each energy balance component to energy loss, using the same colour scheme and flux rates as in (a). Panels (c) and (d) show the equivalent framework for night-time conditions. Absorbed radiation is lower because the only contribution is downward longwave radiation from the sky given the absence of sunshine, while ground heat storage is negative as heat is released from the ground. Latent heat fluxes are smaller because of high stomatal resistance at night (as stomata for most non-CAM plants are typically closed at night), resulting in an equilibrium surface temperature (solid vertical line in d) below air temperature.

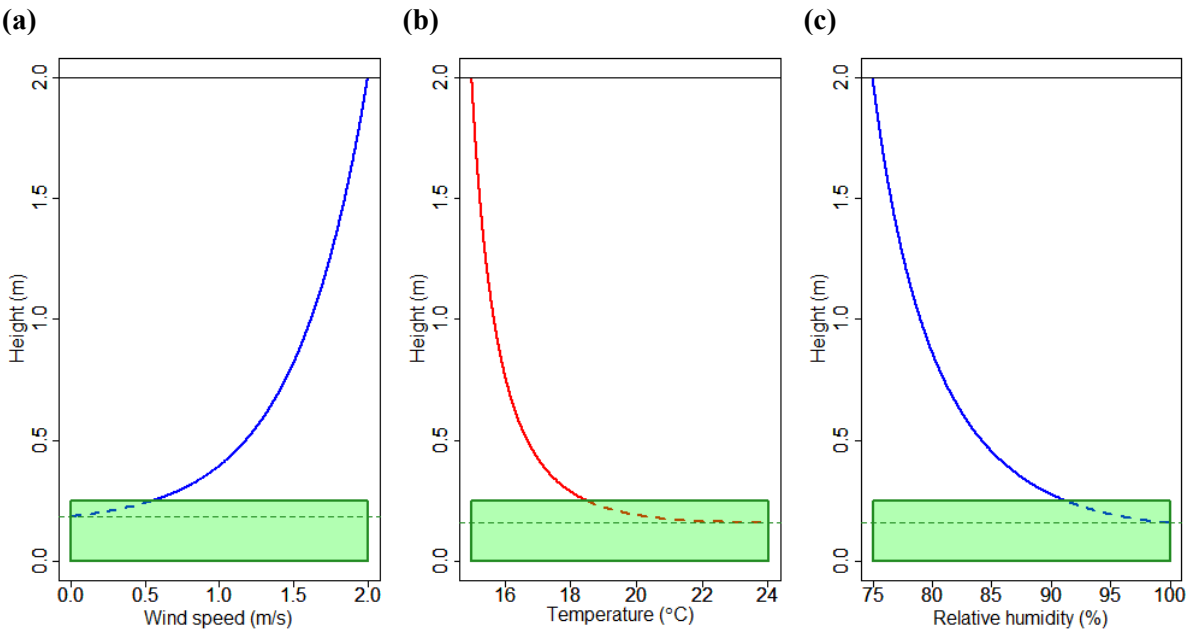

Fig. 2. Typical wind, temperature and relative humidity profiles above a canopy under daytime conditions with positive net radiation at the surface. Areas shaded green indicate the presence of vegetation. Example profiles are shown for daytime conditions with high incoming shortwave radiation and positive net radiation at the surface. In (a), the wind speed profile is shown. The solid line depicts the profile above the canopy and the dashed line its extrapolation towards zero wind speed at a height roughly two-thirds to three quarters of the way to the top of the canopy. In (b), the temperature profile is shown. The solid line depicts the profile above the canopy and the dashed line its extrapolation towards the effective heat exchange surface, representing the notional level within the canopy at which the surface energy balance is solved using the Penman-Monteith equation. In (c), the relative humidity profile is shown. Relative humidity is computed from the vapour pressure profile predicted using the equations presented in Note 4.2 and from the corresponding air temperature profile shown in (b).

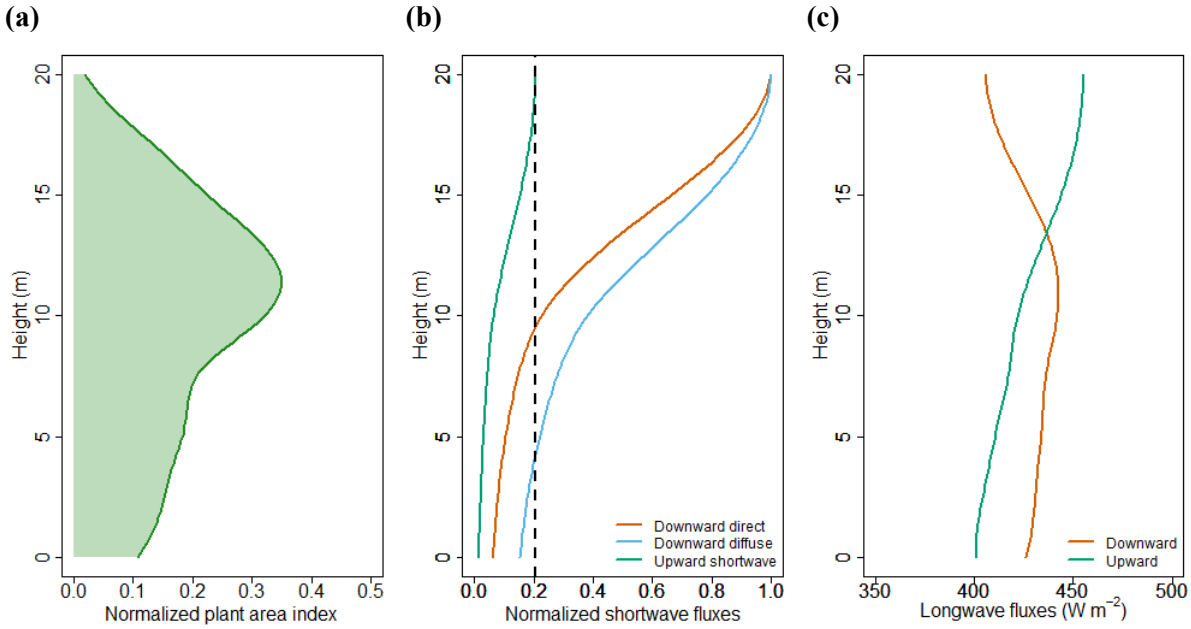

Fig. 3. Typical vertical profiles of radiation fluxes within and below a forest canopy. In (a), an assumed vertical profile of plant area density ($m^2 \cdot m^{-3}$) is shown. In (b), downward direct and diffuse shortwave radiation fluxes, together with the upward shortwave flux, are computed using a two-stream model as described in the text and normalized by the total downward shortwave flux at the top of the canopy. Diffuse radiation is attenuated less strongly than direct radiation because scattering by leaves redistributes radiation within the canopy. The ratio of the upward shortwave flux to the total downward shortwave flux at the top of the canopy (vertical dotted line) gives the surface albedo. In (c), downward and upward longwave radiation fluxes are shown. The downward longwave flux depends on atmospheric emissivity and foliage temperature, whereas the upward flux depends primarily on ground and foliage temperatures.

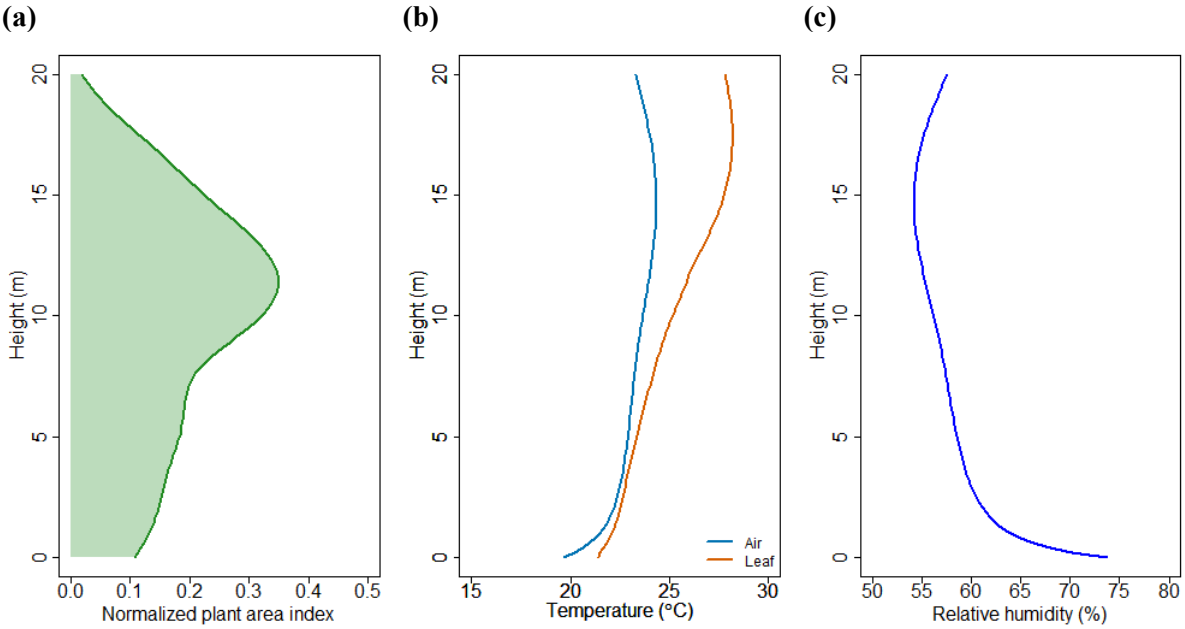

Fig. 4. Typical vertical profiles of daytime temperature and relative humidity below a forest canopy. In (a), an assumed vertical profile of plant area density ($m^2 \cdot m^{-3}$) is shown. In (b), air and leaf temperature profiles computed using Raupach's (1989a,b) localized near-field model are shown, illustrating how temperatures in relatively dense canopies peak near the upper canopy where radiation absorption is greatest. In (c), the air relative humidity profile is shown, determined both by vapour exchange with the ground and foliage and by the temperature profile shown in (b).

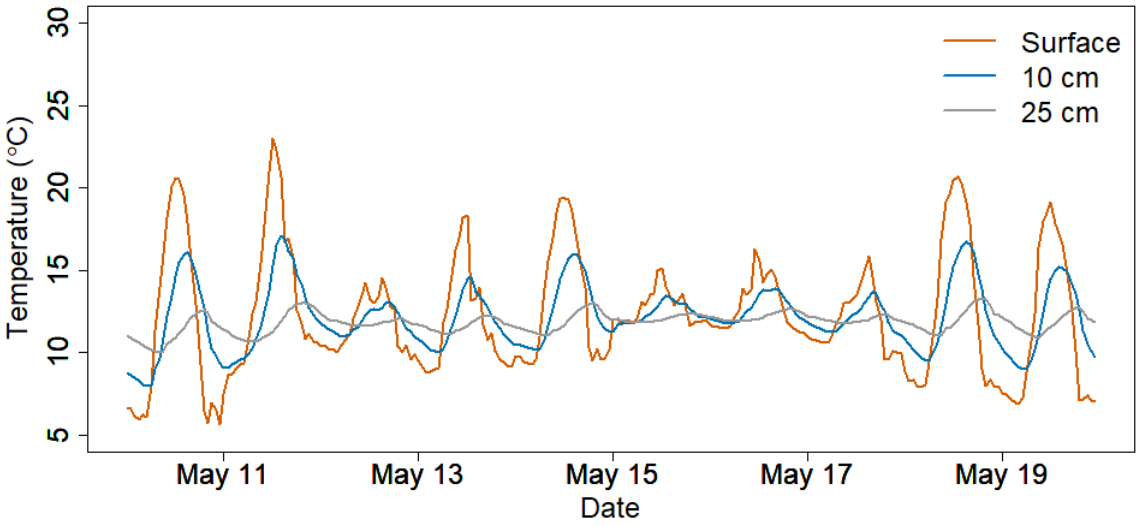

Fig. 5. Modelled soil temperature at the surface and at depths of 10 cm and 25 cm over a 10-day period in May 2017, simulated using the multi-layer coupled soil temperature and water model presented in this tutorial. Simulations for flat unvegetated terrain with a loam soil at Caerthillian Cove, Cornwall, UK (49.968°N, 5.216°W), illustrate the progressive dampening and phase shift of the diurnal temperature cycle with increasing soil depth.